Electronic Research Archive

https://www.aimspress.com/journal/era

ERA, 34(5): 3145–3165.
DOI: 10.3934/era.2026142
Received: 09 February 2026
Revised: 20 March 2026
Accepted: 01 April 2026
Published: 13 April 2026

Research article

Analysis of a stochastic two-patch model with nonlinear birth rate and dispersal driven by the Ornstein–Uhlenbeck process

Beijia Li and Xiaohui Ai*

School of Science, Northeast Forestry University, Harbin 150040, China

* **Correspondence:** Email: axh_826@163.com; Tel: +8618345173579.

Abstract: This paper proposes a novel stochastic two-patch model that incorporates a Beverton–Holt-type nonlinear birth rate and dispersal driven by an Ornstein–Uhlenbeck process. We first establish the existence and uniqueness of a global positive solution, thereby ensuring the biological well–posedness of the model. By constructing appropriate Lyapunov functions and applying Itô's formula, we further demonstrate the existence of a stationary distribution, which characterizes the long-term statistical behavior of the system. Sufficient conditions for population extinction are then derived, providing criteria for predicting when the population is destined to disappear. We perform numerical simulations using the Euler–Maruyama method to validate the main theoretical results. Finally, as an empirical application, the stochastic model achieves a good fit to zooplankton data, confirming its practical validity and offering important insights for mathematical ecology, as well as for species conservation, population regulation, and resource management in fragmented habitats.

Keywords: stochastic two–patch model; Ornstein–Uhlenbeck process; stationary distribution; extinction

1. Introduction

Habitat fragmentation is a primary driver of global biodiversity loss. As human activities increasingly disrupt natural ecosystems, once-contiguous habitats are being subdivided into spatially isolated patches of varying sizes [1]. This fragmentation elevates the risk of local population extinctions, posing a serious threat to species' long-term persistence and the stability of community structures. Consequently, investigating the dynamics of populations in patchy environments—specifically, how species sustain themselves through dispersal in fragmented landscapes—has become a central topic of shared interest in mathematical ecology and conservation biology [1–3]. In particular, [1] provided a systematic review of the effects of habitat fragmentation on populations and elucidated the patterns by which these effects vary with the proportion of suitable habitat; [2] established a theoretical framework for aggregate population ecology, laying the groundwork for research on discrete habitat models; [3] compared the

effects of diffusion on population size in discrete- and continuous-time settings for a two-patch model, identified four response patterns, and deepened our quantitative understanding of diffusion effects.

At the local habitat scale, population dynamics are typically coregulated by multiple density-dependent factors, including resource limitations, intraspecific competition, and the Allee effect. Although traditional linear or constant birth rate assumptions facilitate theoretical analysis, they fall short in reflecting how population birth rates respond to density changes in actual ecological processes. Therefore, a nonlinear birth rate is more ecologically reasonable. As a key ecological process linking spatially separated patches, dispersal serves as a fundamental strategy for species to cope with habitat fragmentation, mitigate local environmental risks, and maintain the stability of metapopulations. Individual movement between patches not only regulates local population sizes but also profoundly influences the persistence and stability of the entire coupled system. As a result, research on population dispersal models is receiving increasing attention from researchers.

In reality, the evolutionary process of populations in real-world environments is often disrupted by various random factors such as temperature, atmospheric oxygen levels, humidity, and light exposure. As May [4] noted, the environmental carrying capacity, intrinsic growth rate, and other system parameters of a population inevitably undergo fluctuations due to environmental noise. Therefore, establishing corresponding mathematical models using stochastic differential equations may represent a more realistic approach. The Ornstein–Uhlenbeck process is a mean-reverting stochastic process, meaning that random fluctuations oscillate around a long-term mean and gradually revert to that baseline level over time. This characteristic closely aligns with ecological reality. It has been extensively studied in the context of stochastic dynamical systems [5, 6]. For instance, Wei [5] analyzed the population dynamics of a two-species Lotka–Volterra competition system by introducing an Ornstein–Uhlenbeck process, and Nie [6] examined the dynamics of a stochastic epidemic model using a similar approach. However, studies on two-patch models that incorporate Ornstein–Uhlenbeck processes remain scarce. To address this gap, our paper constructs a two-patch single species population model driven by an Ornstein–Uhlenbeck process and characterized by nonlinear birth rates and dispersal. It systematically investigates and reveals the synergistic effects of these three factors on the model, thereby contributing to the theoretical understanding of multiple complex interactions in stochastic two-patch systems. The dynamic properties studied fall within the scope of classical research directions , and the findings provide important theoretical references for understanding interspecific interaction mechanisms in ecology and conservation biology.

The remainder of this paper is organized as follows. Section 2 describes the formulation of the model. Section 3 establishes the existence and uniqueness of a global positive solution. Section 4 analyzes the existence of a stationary distribution for the system. Section 5 derives sufficient conditions for population extinction. Section 6 clarifies numerical methods and theoretical justification. Section 7 presents numerical simulations to verify the theoretical results. Section 8 concludes the paper.

2. Model formulation

Population dispersal between patches significantly impacts the survival and development of populations. In recent years, researchers have increasingly focused on studying population dispersal models, with substantial progress made in research on a two-patch single species population with dispersal models [7, 8]. In particular, [7] further examined source–sink population structure, elucidating the multi-

faceted effects of asymmetric dispersal on population size, and establishing the principle that moderate asymmetry promotes population survival, whereas extreme asymmetry tends to lead to extinction. [8] proposed a two-patch single species population model with dispersal incorporating an additive Allee effect, formulated as follows:

$$\begin{cases} \mathrm{d}P(t) = [-(1 + D_1)P(t) + D_2M(t)]\,\mathrm{d}t, \\ \mathrm{d}M(t) = \left[M(t)\left(1 - M(t) - \frac{m}{M(t)+a}\right) + D_1P(t) - D_2M(t)\right]\mathrm{d}t, \end{cases} \tag{2.1}$$

where D_1 (D_2) is the dispersal rate from patch-1(2) to patch-2(1), m and a are Allee effect constants, and $P(t)$ and $M(t)$ represent the population densities of species in patch-1 and patch-2. Their research findings indicate that additive Allee effect and the dispersal rate can lead to either the persistence or extinction of a population. The total population density across both patches increases with higher values of a and D_1, but decreases with higher values of m and D_2. This system exhibits a saddle-node bifurcation.

In ecology, it is well-recognized that the birth rate of a population is influenced by its density. Numerous scholars have argued that incorporating a nonlinear birth rate offers a more realistic representation of population dynamics than other models, and this topic has been the subject of extensive research [9, 10]. Motivated by Model (2.1), we introduce a nonlinear birth rate for the population in the first patch, formulated using the Beverton–Holt function. Specifically, the birth rate is given by $a/(A + P(t))$, which captures the density-dependent regulation of reproduction, where the parameter a denotes the birth rate of patch-1, and A modulates the strength of density dependence. This leads to the following revised model:

$$\begin{cases} \mathrm{d}P(t) = \left[\frac{aP(t)}{A+P(t)} - k(t)P(t) - bP^2(t) - D_1P(t) + D_2M(t)\right]\mathrm{d}t, \\ \mathrm{d}M(t) = [-d_*(t)M(t) + D_1P(t) - D_2M(t)]\,\mathrm{d}t. \end{cases} \tag{2.2}$$

Here, the interaction between the two patches manifests as bidirectional linear diffusion. Specifically, individuals can migrate freely between the two patches at constant rates D_1 and D_2.

Table 1. The meaning of parameters in system (2.2).

Parameter	Description
a	Birth rate of patch-1
A	Density-dependent coefficient of the nonlinear birth rate of patch-1 population
k	Natural mortality rate of patch-1
d_*	Natural mortality rate of patch-2
b	Intraspecific competition rate of patch-1
D_1	Dispersal rate from patch-1 to patch-2
D_2	Dispersal rate from patch-2 to patch-1
$P(t)$	The number of population in patch-1 at time t
$M(t)$	The number of population in patch-2 at time t

Model (2.2) is formulated as a system of ordinary differential equations, assuming all input variables are deterministic functions of time and disregarding the influence of environmental disturbances on these variables. To simulate parameters in a changing environment, two common methods are employed. One

assumes that parameters are subject to perturbations from linear functions of Gaussian white noise. Here, we assume that population birth rates or mortality rates are affected by linear white noise, expressed as

$$a(t) = \bar{a} + \alpha \frac{dB(t)}{dt},$$

where $\bar{a}$, which can be obtained by direct calculation, represents the average value of a over the long term. $B(t)$ is the independent standard Brownian motion defined on a complete probability space $\{\Omega, \mathcal{F}, \{\mathcal{F}_t\}_{t\geq 0}, \mathbb{P}\}$ with the σ-filtration $\{\mathcal{F}_t\}_{t\geq 0}$ satisfying the usual conditions [11], and α denotes the noise density of $B(t)$. From a biological standpoint, this linear white noise is somewhat flawed. This flaw has been mildly criticized by Zhang et al. [12] . Next, we will explain this unreasonable part from both biological and mathematical perspectives. We assume that for any time interval $[0, t]$, $\langle a(t)\rangle$ is the time average of $a(t)$. According to direct calculation, we obtain

$$\langle a(t)\rangle := \frac{1}{t}\int_0^t a(s)ds = \bar{a} + \frac{\alpha B(t)}{t} \sim \mathbb{N}\left(\bar{a}, \frac{\alpha^2}{t}\right),$$

where $\mathbb{N}(\bar{a}, \alpha^2/t)$ is a one-dimensional Gaussian distribution. It is evident that the average state $\langle a(t)\rangle$ on $[0, t]$ has a variance of α^2/t, which approaches infinity as $t \to 0^+$. This leads to an unreasonable outcome where the stochastic fluctuation of the growth rate or mortality rate $a(t)$ becomes very large for a small time interval.

Therefore, we considered another alternative method to simulate random disturbances, namely employing a mean–reverting Ornstein–Uhlenbeck process to model environmental fluctuations. We assume that $k(t)$ and $d_*(t)$ satisfy the Ornstein–Uhlenbeck process; then, we have

$$\mathrm{d}k(t) = \left[\alpha_1(\bar{k} - k(t))\right]\mathrm{d}t + \sigma_1 \mathrm{d}B_1(t),\ \mathrm{d}d_*(t) = \left[\alpha_2(\bar{d}_* - d_*(t))\right]\mathrm{d}t + \sigma_2 \mathrm{d}B_2(t), \tag{2.3}$$

where $\bar{k}$ and $\bar{d}_*$ represent the average levels of $k(t)$ and $d_*(t)$, respectively; σ_i $(i = 1, 2)$ are the intensities of volatility; α_i $(i = 1, 2)$ are the speeds of reversion; and σ_i and α_i are all positive constants. $B_i(t)$ are mutually independent standard Brownian motions on the complete probability space $(\Omega, \mathcal{F}, \{\mathcal{F}_t\}_{t\geq 0}, \mathbb{P})$. Integrating Eq (2.3) over the interval $[0, t]$ yields the following corresponding explicit solution:

$$k(t) = \bar{k} + \left(k^0 - \bar{k}\right)e^{-\alpha_1 t} + \sigma_1 \int_0^t e^{-\alpha_1(t-s)} dB_1(s), d_*(t) = \bar{d}_* + \left(d_*^0 - \bar{d}_*\right)e^{-\alpha_2 t} + \sigma_2 \int_0^t e^{-\alpha_2(t-s)} dB_2(s),$$

where $k^0 = k(0)$ and $d_*^0 = d_*(0)$ are the initial values of $k(t)$ and $d_*(t)$. Their expectations and variances are:

$$\mathbb{E}\left[k(t)\right] = \bar{k} + \left(k^0 - \bar{k}\right)e^{-\alpha_1 t}, \mathbb{E}\left[d_*(t)\right] = \bar{d}_* + \left(d_*^0 - \bar{d}_*\right)e^{-\alpha_2 t},$$
$$\mathrm{Var}\left[k(t)\right] = \sigma_1^2(1 - e^{-2\alpha_1 t})/2\alpha_1, \mathrm{Var}\left[d_*(t)\right] = \sigma_2^2(1 - e^{-2\alpha_2 t})/2\alpha_2.$$

From the properties of Brownian motion, it is readily derived that $\sigma_1 \int_0^t e^{-\alpha_1(t-s)}\mathrm{d}B_1(s)$ follows a normal distribution $\mathbb{N}(0, \sigma_1^2(1 - e^{-2\alpha_1 t})/(2\alpha_1))$, and $k(t)$ follows a normal distribution $\mathbb{N}(\bar{k} + (k^0 - \bar{k})e^{-\alpha_1 t}, \sigma_1^2(1 - e^{-2\alpha_1 t})/(2\alpha_1))$, where $t \to \infty$, $k(t)$ follows a normal distribution $\mathbb{N}(k^0, 0)$. Similarly, $d^*(t)$ shares the same properties as $k(t)$.

Therefore, within a certain time interval, the fluctuations of $k(t)$ and $d^*(t)$ remain within a relatively small range, consistent with the continuous disturbance characteristics of environmental

noise. This indicates that employing the Ornstein–Uhlenbeck process to model random disturbances is reasonable [13]. By combining Eqs (2.2) and (2.3) and setting $q_1(t) = k(t) - \bar{k}$, $q_2(t) = d_*(t) - \bar{d}_*$, we thus obtain the following single species two-patch model with nonlinear birth rates and dispersal driven by Ornstein–Uhlenbeck processes:

$$\begin{cases} \mathrm{d}P(t) = \left[\frac{aP(t)}{A+P(t)} - (q_1(t) + \bar{k})P(t) - bP^2(t) - D_1P(t) + D_2M(t)\right]\mathrm{d}t, \\ \mathrm{d}M(t) = \left[-(q_2(t) + \bar{d}_*)M(t) + D_1P(t) - D_2M(t)\right]\mathrm{d}t, \\ \mathrm{d}q_1(t) = -\alpha_1 q_1(t)\mathrm{d}t + \sigma_1 \mathrm{d}B_1(t), \\ \mathrm{d}q_2(t) = -\alpha_2 q_2(t)\mathrm{d}t + \sigma_2 \mathrm{d}B_2(t). \end{cases} \tag{2.4}$$

3. Existence and uniqueness of the global solution

To investigate the long-term dynamic behavior of a single species two-patch model system, it is first necessary to ensure that Model (2.4) possesses a unique global solution. Therefore, we will present the existence and uniqueness theorem for the global solution of the Model (2.4).

Theorem 3.1. *For any given initial value* $(P(0), M(0), q_1(0), q_2(0))^{\mathrm{T}} \in \mathbb{R}^2_+ \times \mathbb{R}^2$*, when* $t > 0$*, the Model* (2.4) *possesses a unique global solution, and this solution will exist with probability* 1.

Proof. First, we verify that System (2.4) satisfies the local Lipschitz condition and linear growth condition on $\mathbb{R}^2_+ \times \mathbb{R}^2$. By the classical existence and uniqueness theorem for stochastic differential equations, there exists a unique local solution $(P(t), M(t), q_1(t), q_2(t))$ defined on $[0, \tau_e)$, where τ_e is the explosion time. It suffices to show that $\tau_e = \infty$.

Let n be sufficiently large such that $P(0), M(0) \in (e^{-n}, e^n)$, and $q_1(0), q_2(0) \in (-n, n)$. Define the stopping time

$$\tau_n = \inf\{t \in [0, \tau_e] : \ln P(t) \notin (-n, n) \text{ or } \ln M(t) \notin (-n, n) \text{ or } q_1(t) \notin (-n, n) \text{ or } q_2(t) \notin (-n, n)\},$$

which is monotonically increasing as $n \to \infty$. Set $\tau_\infty = \lim_{n\to\infty} \tau_n$; then, $\tau_\infty \le \tau_e$. We only need to prove $\tau_\infty = \infty$. Suppose for contradiction that $\tau_\infty < \infty$; then, there exist $T > 0$ and $\varepsilon \in (0, 1)$ such that $\mathbb{P}\{\tau_\infty \le T\} > \varepsilon$. Thus, there exists an integer $n_1 > n_0$ such that

$$\mathbb{P}\{\tau_n \le T\} \ge \varepsilon, \quad \forall n \ge n_1.$$

Define a C^2 function $V_0(P, M, q_1, q_2)$ of the following form:

$$V_0(P, M, q_1, q_2) = P - 1 - \ln P + M - 1 - \ln M + \frac{1}{4}q_1^4 + \frac{1}{4}q_2^4. \tag{3.1}$$

Applying Itô's formula to V_0 yields:

$$dV_0 = \mathcal{L}V_0(P, M, q_1, q_2)dt + q_1^3\sigma_1 dB_1(t) + q_2^3\sigma_2 dB_2(t),$$

where

$$\begin{aligned} \mathcal{L}V_0 = {} & \frac{aP}{A+P} - \bar{k}P - q_1P - bP^2 - \frac{a}{A+P} + \bar{k} + q_1 + bP + D_1 - \frac{D_2M}{P} \\ & - q_2M - \bar{d}_*M - \frac{D_1P}{M} + D_2 + q_2 + \bar{d}_* - \alpha_1 q_1^4 - \alpha_2 q_2^4 + \frac{3}{2}\sigma_1^2 q_1^2 + \frac{3}{2}\sigma_2^2 q_2^2. \end{aligned}$$

Applying Young's inequality gives

$$-q_1P \le P|q_1| \le \frac{2}{3}P^{\frac{3}{2}} + \frac{1}{3}|q_1|^3.$$

Noting that $q_2M + \bar{d}_*M = d_*M$, we obtain

$$\begin{aligned}\mathcal{L}V_0 \le{}& \frac{a}{A}P - \bar{k}P + \frac{2}{3}P^{\frac{3}{2}} + \frac{1}{3}|q_1|^3 - bP^2 - \frac{a}{A+P} + \bar{k} + q_1 + bP + D_1 - 2\sqrt{D_1D_2} - \bar{d}_*M - q_2M \\ &+ D_2 + q_2 + \bar{d}_* - \alpha_1 q_1^4 - \alpha_2 q_2^4 + \frac{3}{2}\sigma_1^2 q_1^2 + \frac{3}{2}\sigma_2^2 q_2^2 \\ \le{}& \sup_{(P,M)\in\mathbb{R}_+^2}\left[-bP^2 + \frac{2}{3}P^{\frac{3}{2}} + \frac{a}{A}P - \bar{k}P + bP - \frac{a}{A+P} - d_*M + \bar{k} + \bar{d}_* + D_1 + D_2 - 2\sqrt{D_1D_2}\right] \\ &+ \sup_{(q_1,q_2)\in\mathbb{R}^2}\left(-\alpha_1 q_1^4 + \frac{1}{3}|q_1|^3 + \frac{3}{2}\sigma_1^2 q_1^2 + q_1 - \alpha_2 q_2^4 + \frac{3}{2}\sigma_2^2 q_2^2 + q_2\right) \le G,\end{aligned} \tag{3.2}$$

where G is a positive constant.

Integrating both sides of the inequality $dV_0 \le Gdt + q_1^3\sigma_1 dB_1(t) + q_2^3\sigma_2 dB_2(t)$ from 0 to $\tau_n \wedge T$ and taking expectations, we get

$$\mathbb{E}\left[V_0(P(\tau_n \wedge T), M(\tau_n \wedge T), q_1(\tau_n \wedge T), q_2(\tau_n \wedge T))\right] \le V_0(P(0), M(0), q_1(0), q_2(0)) + GT.$$

Let $\Omega_n = \{\tau_n \le T\}$. Then, $\mathbb{P}(\Omega_n) \ge \varepsilon$. Notice that for any $\omega \in \Omega_n$, there exists at least one component touching the boundary, so

$$V_0(P(\tau_n,\omega), M(\tau_n,\omega), q_1(\tau_n,\omega), q_2(\tau_n,\omega)) \ge \varepsilon \min\left\{e^n - 1 - n, e^{-n} - 1 + n, \frac{n^4}{4}\right\}.$$

Taking expectations yields

$$\mathbb{E}\left[1_{\Omega_n}(\omega)V_0(P(\tau_n,\omega), M(\tau_n,\omega), q_1(\tau_n,\omega), q_2(\tau_n,\omega))\right] \ge \varepsilon \min\left\{e^n - 1 - n, e^{-n} - 1 + n, \frac{n^4}{4}\right\}.$$

As $n \to \infty$, the right-hand side tends to infinity, whereas the left-hand side is bounded by $V_0(P(0), M(0), q_1(0), q_2(0)) + GT < \infty$, which leads to a contradiction. Therefore, $\tau_\infty = \infty$, which implies $\tau_e = \infty$.

Hence, Model (2.4) has a unique global solution for any initial value $(P(0), M(0), q_1(0), q_2(0)) \in \mathbb{R}_+^2 \times \mathbb{R}^2$, and this solution will exist with probability 1. □

4. Existence of a stationary distribution

The existence of a stationary distribution implies the long-term coexistence of the population. To further investigate the survival of this system, the existence of a stationary distribution for Model (2.4) will be discussed. Let $X(t)$ denote a given homogeneous Markov process in $\mathbb{R}^d$. Consider the following stochastic differential equation:

$$dX(t) = \zeta(X(t))dt + \sum_{i=1}^{k}\vartheta_i(X(t))dB_i(t). \tag{4.1}$$

Lemma 4.1. *[14] Suppose the vectors $\zeta(X), \vartheta_1(X), \ldots, \vartheta_k(X)$ $(t \geq t_0, X \in \mathbb{R}^d)$ are continuous functions of $X(t)$, which satisfy the following conditions:*

(1) There exists a constant ρ such that

$$|\zeta(X_1) - \zeta(X_2)| + \sum_{i=1}^{k} |\vartheta_i(X_1) - \vartheta_i(X_2)| \leq \rho |X_1 - X_2|, \ |\zeta(X)| + \sum_{i=1}^{k} |\vartheta_i(X)| \leq \rho(1 + |X|).$$

(2) If there exists a non-negative C^2 function $U(x) \subset \mathbb{R}^d$ such that $\mathcal{L}U(x) \leq -1$ holds outside a bounded closed set, then the solution $X(t)$ of Eq (4.1) *is a stationary Markov process.*

Because the rates of local processes (births, deaths, and intraspecific competition) are much faster than spatial dispersal, the population rapidly reaches a transient equilibrium, effectively erasing historical information. This forms the basis for the ecologically plausible Markovian nature of this model (see [15] for details).

Theorem 4.1. *If $2\sqrt{D_1 D_2} - \bar{k} - \bar{d}_* - \sigma_1/\sqrt{\pi\alpha_1} - \sigma_2/\sqrt{\pi\alpha_2} > 0$, then there exists a stationary distribution $\pi(\cdot)$ for Model* (2.4) *in $\mathbb{R}^2_+ \times \mathbb{R}^2$.*

Proof. As noted in [16], Annotation 5 confirms that Theorem 3.1 holds, meaning that Condition (1) is satisfied. Below, we will verify in three steps that Condition (2) is also satisfied.
Step 1. Define a C^2 function $V(P, M, q_1, q_2) : \mathbb{R}^2_+ \times \mathbb{R}^2 \to \mathbb{R}$ as follows:

$$V(P, M, q_1, q_2) = \tilde{V}(P, M, q_1, q_2) - \tilde{V}(P_0, M_0, q_{10}, q_{20}) =$$

$$V_2(P, M, q_1, q_2) + V_3(P, M, q_1, q_2) - \tilde{V}(P_0, M_0, q_{10}, q_{20}),$$

where

$$V_2(P, M, q_1, q_2) = \xi\left(-\ln P - \ln M - \frac{q_1}{\alpha_1} - \frac{q_2}{\alpha_2}\right), \quad V_3(P, M, q_1, q_2) = P + M + \frac{1}{4}q_1^4 + \frac{1}{4}q_2^4.$$

□

Note that $\tilde{V}(P, M, q_1, q_2)$ is continuous, and as $(P, M, q_1, q_2)^T$ approaches the boundary of ${\mathbb{R}_+}^2 \times \mathbb{R}^2$, $\tilde{V}(P, M, q_1, q_2)$ tends to ∞, where $\tilde{V}(P_0, M_0, q_{10}, q_{20})$ is the lower bound of $\tilde{V}(P, M, q_1, q_2)$. Applying Itô's formula to V_2,

$$\begin{aligned}\mathcal{L}V_2 = \xi\left[-\frac{a}{A+P} - \frac{D_1 M}{P} + \bar{k} + bP - \frac{D_2 P}{M} + \bar{d}_* + D_1 + D_2 + 2(q_1 + q_2)\right] \leq \\ \xi\left(D_1 + D_2 - 2\sqrt{D_1 D_2} + \bar{k} + \bar{d}_* + bP + 2q_1 + 2q_2\right) \leq \\ -\xi\bar{\omega} + \xi\left(bP + D_1 + D_2\right) + \xi[2(q_1 \vee 0) + 2(q_2 \vee 0)],\end{aligned}$$

where $\bar{\omega} = 2\sqrt{D_1 D_2} - \bar{k} - \bar{d}_*$, we recall the ergodicity of q_1 and q_2 from Section 5,

$$\int_{-\infty}^{\infty} (q_i \vee 0)\omega_i(q)\mathrm{d}q = \int_0^{\infty} \frac{q\sqrt{\alpha_i}}{\sqrt{\pi}\sigma_i} \mathrm{e}^{-\frac{\alpha_i q^2}{\sigma_i^2}} \mathrm{d}q = \frac{\sigma_i}{2\sqrt{\pi\alpha_i}} \int_0^{\infty} \mathrm{e}^{-\left(\frac{\sqrt{\alpha_i}q}{\sigma_i}\right)^2} \mathrm{d}\left(\frac{\sqrt{\alpha_i}q}{\sigma_i}\right)^2 = \frac{\sigma_i}{2\sqrt{\pi\alpha_i}}. \tag{4.2}$$

we then obtain

$$\begin{aligned}\mathcal{L}V_2 \leq & -\xi\bar{\omega} + \xi\left(bP + D_1 + D_2\right) + \xi\left(\frac{2\sigma_1}{2\sqrt{\pi\alpha_1}} + \frac{2\sigma_2}{2\sqrt{\pi\alpha_2}}\right) + 2\xi\left[(q_1 \vee 0) - \int_{-\infty}^{\infty}(q \vee 0)\omega_1(q)\,\mathrm{d}q\right] \\ & + 2\xi\left[(q_2 \vee 0) - \int_{-\infty}^{\infty}(q \vee 0)\omega_2(q)\,\mathrm{d}q\right] \\ \leq & -\xi\bar{\omega}_1 + \xi\left(bP + D_1 + D_2\right) + 2\xi\left[(q_1 \vee 0) - \int_{-\infty}^{\infty}(q \vee 0)\omega_1(q)\,\mathrm{d}q\right] \\ & + 2\xi\left[(q_2 \vee 0) - \int_{-\infty}^{\infty}(q \vee 0)\omega_2(q)\,\mathrm{d}q\right],\end{aligned} \tag{4.3}$$

where $\overline{\omega}_1 = 2\sqrt{D_1D_2} - \bar{k} - \bar{d}_* - \sqrt{\sigma_1^2/(\pi\alpha_1)} - \sqrt{\sigma_2^2/(\pi\alpha_2)} > 0$. Then, applying Itô's formula and Young's inequality to V_3 gives

$$\begin{aligned}\mathcal{L}V_3 = & \left[\frac{aP}{A+P} - (q_1 + \bar{k})P - bP^2 - D_1P + D_2M\right] + \left[-(q_2 + \bar{d}_*)M + D_1P - D_2M\right] - \alpha_1q_1^4 - \alpha_2q_2^4 \\ & + \frac{3}{2}q_1^2\sigma_1^2 + \frac{3}{2}q_2^2\sigma_2^2 \leq \frac{a}{A}P + |q_1|P - \bar{k}P - bP^2 - d_*M - \alpha_1q_1^4 - \alpha_2q_2^4 + \frac{3}{2}q_1^2\sigma_1^2 + \frac{3}{2}q_2^2\sigma_2^2 \\ & \leq \frac{a}{A}P + \frac{2}{3}P^{\frac{3}{2}} + \frac{1}{3}|q_1|^3 - \bar{k}P - bP^2 - d_*M - \alpha_1q_1^4 - \alpha_2q_2^4 + \frac{3}{2}q_1^2\sigma_1^2 + \frac{3}{2}q_2^2\sigma_2^2.\end{aligned} \tag{4.4}$$

Reviewing Eqs (4.3) and (4.4), we derive

$$\begin{aligned}\mathcal{L}V \leq & -\xi\overline{\omega}_1 + Q_1 + \xi(bP + D_1 + D_2) + 2\xi\left[(q_1 \vee 0) - \int_{-\infty}^{\infty}(q \vee 0)\omega_1(q)\mathrm{d}q\right] + \\ & 2\xi\left[(q_2 \vee 0) - \int_{-\infty}^{\infty}(q \vee 0)\omega_2(q)\mathrm{d}q\right] - \frac{1}{2}bP^2 - \frac{1}{2}\alpha_1q_1^4 - \frac{1}{2}\alpha_2q_2^4,\end{aligned} \tag{4.5}$$

where

$$Q_1 = \sup_{(P,M,q_1,q_2)\in\mathbb{R}_+^2\times\mathbb{R}^2}\left\{-\frac{1}{2}bP^2 + \frac{2}{3}P^{\frac{3}{2}} + \frac{a}{A}P - \bar{k}P - \frac{1}{2}\alpha_1q_1^4 + \frac{1}{3}|q_1|^3 - \frac{1}{2}\alpha_2q_2^4 + \frac{3}{2}q_1^2\sigma_1^2 + \frac{3}{2}q_2^2\sigma_2^2\right\}.$$

Next, selecting a sufficiently large constant $\xi > 0$ such that $-\xi\bar{\omega}_1 + Q_1 \leq -2$, from Eq (4.5), we obtain

$$\begin{aligned}\mathcal{L}V \leq & -\xi\overline{\omega}_1 + Q_1 + \xi(bP + D_1 + D_2) + 2\xi\left[(q_1 \vee 0) - \int_{-\infty}^{\infty}(q \vee 0)\omega_1(q)\mathrm{d}q\right] + \\ & 2\xi\left[(q_2 \vee 0) - \int_{-\infty}^{\infty}(q \vee 0)\omega_2(q)\mathrm{d}q\right] - \frac{1}{2}bP^2 - d_*M - \frac{1}{2}\alpha_1q_1^4 - \frac{1}{2}\alpha_2q_2^4 \leq \\ & -2 + \xi(bP + D_1 + D_2) + 2\xi\left[(q_1 \vee 0) - \int_{-\infty}^{\infty}(q \vee 0)\omega_1(q)\mathrm{d}q\right] + \\ & 2\xi\left[(q_2 \vee 0) - \int_{-\infty}^{\infty}(q \vee 0)\omega_2(q)\mathrm{d}q\right] - \frac{1}{2}bP^2 - d_*M - \frac{1}{2}\alpha_1q_1^4 - \frac{1}{2}\alpha_2q_2^4 = \\ & F_1(P, M, q_1, q_2) + 2\xi\left[(q_1 \vee 0) - \int_{-\infty}^{\infty}(q \vee 0)\omega_1(q)\mathrm{d}q\right] + \\ & 2\xi\left[(q_2 \vee 0) - \int_{-\infty}^{\infty}(q \vee 0)\omega_2(q)\mathrm{d}q\right],\end{aligned} \tag{4.6}$$

where

$$F_1 = -2 + \xi(bP + D_1 + D_2) - \frac{1}{2}bP^2 - d_*M - \frac{1}{2}\alpha_1 q_1^4 - \frac{1}{2}\alpha_2 q_2^4.$$

Step 2: Considering a closed set $\mathbb{H}_\varepsilon$, the form

$$\mathbb{H}_\varepsilon = \left\{(P, M, q_1, q_2)^\top \in \mathbb{R}_+^2 \times \mathbb{R}^2 \mid \frac{1}{\varepsilon} \geq P \geq \varepsilon,\ \frac{1}{\varepsilon^2} \geq M \geq \varepsilon^2,\ |q_1| \leq \frac{1}{\varepsilon},\ |q_2| \leq \frac{1}{\varepsilon}\right\} :=$$

$$\overline{\mathbb{H}_\varepsilon} \times \left[-\frac{1}{\varepsilon}, \frac{1}{\varepsilon}\right] \times \left[-\frac{1}{\varepsilon}, \frac{1}{\varepsilon}\right],$$

where $\overline{\mathbb{H}_\varepsilon} = \left\{(P, M, q_1, q_2)^\top \in \mathbb{R}_+^2 \times \mathbb{R}^2 \mid \frac{1}{\varepsilon} \geq P \geq \varepsilon,\ \frac{1}{\varepsilon^2} \geq M \geq \varepsilon^2\right\}$. Let $\varepsilon \in (0, 1)$ be a sufficiently small number, such that the following inequalities hold:

$$-2 + \frac{1}{4}b\varepsilon^2 + Q_2 \leq -1, \tag{4.7}$$

$$-2 + Q_3 - \alpha_1/4\varepsilon^4 \leq -1, \tag{4.8}$$

$$-2 + Q_3 - \alpha_2/4\varepsilon^4 \leq -1, \tag{4.9}$$

$$-2 + Q_2 - \frac{1}{4}b\varepsilon^2 \leq -1. \tag{4.10}$$

Here, Q_2 and Q_3 will be determined in the subsequent proof. Decompose $\mathbb{R}_+^2 \times \mathbb{R}^2 \setminus \mathbb{H}_\varepsilon$ into six subsets $D_{\varepsilon,i}^c$ $(i = 1, \ldots, 6)$ as follows:

$$\mathbb{H}_{\varepsilon,1}^c = \{P < \varepsilon\}, \quad \mathbb{H}_{\varepsilon,2}^c = \{M < \varepsilon^2\}, \quad \mathbb{H}_{\varepsilon,3}^c = \{|q_1| > 1/\varepsilon\},$$
$$\mathbb{H}_{\varepsilon,4}^c = \{|q_2| > 1/\varepsilon\}, \quad \mathbb{H}_{\varepsilon,5}^c = \{P > 1/\varepsilon\}, \quad \mathbb{H}_{\varepsilon,6}^c = \{M > 1/\varepsilon^2\}.$$

Next, we verify that $F_1(P, M, q_1, q_2) \leq -1$ holds in $\mathbb{R}_+^2 \times \mathbb{R}^2 \setminus \mathbb{H}_\varepsilon$ by considering six cases separately. **Case 1.** If (P, M, q_i) is located in the set defined by $\mathbb{H}_{(1,\varepsilon)}^c$, then one can obtain the corresponding results by combining Eqs (4.6) and (4.7).

$$\begin{aligned} F_1(P, M, q_1, q_2) &\leq -2 + Q_2 - d_*M - \frac{1}{4}bP^2 - \frac{1}{4}\alpha_1 q_1^4 - \frac{1}{4}\alpha_2 q_2^4 \\ &\leq -2 + Q_2 + \frac{1}{4}bP^2 \leq -2 + Q_2 + \frac{1}{4}b\varepsilon^2 \leq -1. \end{aligned} \tag{4.11}$$

where

$$Q_2 = \sup_{(P,M,q_1,q_2)^\top \in \mathbb{R}_+^2 \times \mathbb{R}^2 \setminus \mathbb{H}_\varepsilon} \left\{\xi(bP + D_1 + D_2) - \frac{1}{4}bP^2 - \frac{1}{4}\alpha_1 q_1^4 - \frac{1}{4}\alpha_2 q_2^4\right\} < \infty.$$

Case 2. If (P, M, q_i) is located in the set defined by $\mathbb{H}_{(2,\varepsilon)}^c$, consequently, from Eqs (4.6) and (4.7), we can obtain the relevant result:

$$\begin{aligned} F_1(P, M, q_1, q_2) &\leq -2 + Q_2 - d_*M - \frac{1}{4}bP^2 - \frac{1}{4}\alpha_1 q_1^4 - \frac{1}{4}\alpha_2 q_2^4 \\ &\leq -2 + Q_2 - d_*M \leq -2 + Q_2 + \frac{1}{4}b\varepsilon^2 \leq -1. \end{aligned} \tag{4.12}$$

Case 3. For any (P, M, q_i), which is located in the set defined in $\mathbb{H}^c_{(\varepsilon,3)}$, according to Eqs (4.6) and (4.8), we obtain

$$\begin{aligned} F_1(P, M, q_1, q_2) &\leq -2 + Q_3 - \frac{1}{4}bP^2 - \frac{1}{4}\alpha_1 q_1^4 - \frac{1}{4}\alpha_2 q_2^4 \\ &\leq -2 + Q_3 - \frac{1}{4}\alpha_1 q_1^4 \leq -2 + Q_3 - \frac{\alpha_1}{4\varepsilon^4} \leq -1, \end{aligned} \tag{4.13}$$

where

$$Q_3 = \sup_{(P,M,q_1,q_2)^\top \in \mathbb{R}^2_+ \times \mathbb{R}^2 \setminus \mathbb{H}_\varepsilon} \left\{ \xi(bP + D_1 + D_2) - d_* M - \frac{1}{4}bP^2 - \frac{1}{4}\alpha_1 q_1^4 - \frac{1}{4}\alpha_2 q_2^4 \right\} < \infty.$$

Case 4. In the event that (P, M, q_i) is situated within the set defined by $\mathbb{H}^c_{(4,\varepsilon)}$, the associated findings can be calculated by Eqs (4.6) and (4.9).

$$\begin{aligned} F_1(P, M, q_1, q_2) &\leq -2 + Q_3 - \frac{1}{4}bP^2 - \frac{1}{4}\alpha_1 q_1^4 - \frac{1}{4}\alpha_2 q_2^4 \\ &\leq -2 + Q_3 - \frac{1}{4}\alpha_2 q_2^4 \leq -2 + Q_3 - \frac{\alpha_2}{4\varepsilon^4} \leq -1. \end{aligned} \tag{4.14}$$

Case 5. If (P, M, q_i) is situated within the set defined by $\mathbb{H}^c_{(5,\varepsilon)}$, it follows from Eqs (4.6) and (4.10).

$$F_1(P, M, q_1, q_2) \leq -2 + Q_2 - \frac{1}{4}bP^2 - \frac{1}{4}\alpha_1 q_1^4 - \frac{1}{4}\alpha_2 q_2^4 \leq -2 + Q_2 - \frac{b}{4\varepsilon^2} \leq -1. \tag{4.15}$$

Case 6. If (P, M, q_i) lies within the set demarcated by $\mathbb{H}^c_{(\varepsilon,6)}$, the relevant conclusion is deduced through Eqs (4.6) and (4.7).

$$\begin{aligned} F_1(P, M, q_1, q_2) &\leq -2 + Q_2 - d_* M - \frac{1}{4}bP^2 - \frac{1}{4}\alpha_1 q_1^4 - \frac{1}{4}\alpha_2 q_2^4 \\ &\leq -2 + Q_2 - d_* M \leq -2 + Q_2 + \frac{1}{4}b\varepsilon^2 \leq -1. \end{aligned} \tag{4.16}$$

Based on the above six scenarios, it follows that for any$(P, M, q_1, q_2)^\top \in \mathbb{R}^2_+ \times \mathbb{R}^2 \setminus \mathbb{H}_\varepsilon$, there exists a sufficiently small ε such that

$$F_1(P, M, q_1, q_2) \leq -1. \tag{4.17}$$

Let

$$G_1 = \sup_{(P,M,q_1,q_2) \in \mathbb{R}^2_+ \times \mathbb{R}^2} \left\{ -2 + \varepsilon(bP + D_1 + D_2) - \frac{1}{2}bP^2 - \frac{1}{2}\alpha_1 q_1^4 - \frac{1}{2}\alpha_2 q_2^4 \right\}. \tag{4.18}$$

so that we can obtain

$$F_1(P, M, q_1, q_2) \leq G_1 < +\infty, \ \forall (P, M, q_1, q_2)^\top \in \mathbb{R}^2_+ \times \mathbb{R}^2. \tag{4.19}$$

Reviewing Eq (4.6) yields

$$\mathcal{L}V \leq F_1(P, M, q_1, q_2) + 2\xi[(q_1 \vee 0) - \int_{-\infty}^{\infty} (q \vee 0)\omega_1(q)\mathrm{d}q] + 2\xi\,(q_2 \vee 0) - \int_{-\infty}^{\infty} (q \vee 0)\omega_2(q)\mathrm{d}q. \tag{4.20}$$

Step 3: Existence

For any initial value $(P(0), M(0), q_1(0), q_2(0))^\top \in \mathbb{R}^2_+ \times \mathbb{R}^2$ and the interval $[0, t]$, applying Itô's formula and expectation to $V(P, M, q_1, q_2)$ results in

$$\begin{aligned}
&0 \le \frac{\mathbb{E}V(P(t), M(t), q_1(t), q_2(t))}{t} = \frac{\mathbb{E}V(P(0), M(0), q_1(0), q_2(0))}{t} + \\
&\frac{1}{t}\int_0^t \mathbb{E}(\mathcal{L}V(P(\tau), M(\tau), q_1(\tau), q_2(\tau)))\mathrm{d}\tau \le \frac{\mathbb{E}V(P(0), M(0), q_1(0), q_2(0))}{t} + \\
&\frac{1}{t}\int_0^t \mathbb{E}(F_1(P(\tau), M(\tau), q_1(\tau), q_2(\tau)))\mathrm{d}\tau + 2\xi\mathbb{E}\left[\frac{1}{t}\int_0^t (q_1(\tau) \vee 0)\mathrm{d}\tau - \int_{-\infty}^{\infty}(q \vee 0)\omega_1(q)\mathrm{d}q\right] + \\
&2\xi\mathbb{E}\left[\frac{1}{t}\int_0^t (q_2(\tau) \vee 0)\mathrm{d}\tau - \int_{-\infty}^{\infty}(q \vee 0)\omega_2(q)\mathrm{d}q\right].
\end{aligned} \tag{4.21}$$

Then, using the ergodicity and the strong law of large numbers for $q_i(t)$ $(i = 1, 2)$, we obtain

$$\lim_{t\to+\infty} \mathbb{E}\left[\frac{1}{t}\int_0^t (q_i(\tau) \vee 0)\mathrm{d}\tau - \int_{-\infty}^{\infty}(q \vee 0)\omega_i(q)\mathrm{d}q\right] = \mathbb{E}\left[\int_0^{\infty} q\omega_i(q)\mathrm{d}q\right] - \int_0^{\infty} q\omega_i(q)\mathrm{d}q = 0 \text{ a.s.} \tag{4.22}$$

As $t \to +\infty$, taking the lower limit on both sides of Eq (4.21) and combining it with Eq (4.22) yields

$$\begin{aligned}
&0 \le \liminf_{t\to+\infty} \frac{\mathbb{E}V(P(0), M(0), q_1(0), q_2(0))}{t} + \liminf_{t\to+\infty} \frac{1}{t}\int_0^t \mathbb{E}\left[F_1(P(\tau), M(\tau), q_1(\tau), q_2(\tau))\right]\mathrm{d}\tau + \\
&\lim_{t\to+\infty}\left\{2\xi\mathbb{E}\left[\frac{1}{t}\int_0^t (q_1(\tau) \vee 0)\mathrm{d}\tau - \int_{-\infty}^{\infty}(q \vee 0)\omega_1(q)\mathrm{d}q\right] + \right. \\
&\left. 2\xi\mathbb{E}\left[\frac{1}{t}\int_0^t (q_2(\tau) \vee 0)\mathrm{d}\tau - \int_{-\infty}^{\infty}(q \vee 0)\omega_2(q)\mathrm{d}q\right]\right\} = \\
&\liminf_{t\to+\infty} \frac{1}{t}\int_0^t \mathbb{E}\left[F_1(P(\tau), M(\tau), q_1(\tau), q_2(\tau))\right]\mathrm{d}\tau \text{ a.s.}
\end{aligned} \tag{4.23}$$

Subsequently, combining Eqs (4.19) and (4.20) gives

$$\begin{aligned}
&\liminf_{t\to+\infty} \frac{1}{t}\int_0^t \mathbb{E}\left(F_1(P(\tau), M(\tau), q_1(\tau), q_2(\tau))\right)\mathrm{d}\tau = \\
&\liminf_{t\to+\infty} \frac{1}{t}\int_0^t \mathbb{E}\left[F_1(P(\tau), M(\tau), q_1(\tau), q_2(\tau))\right] 1_{\{(P(\tau), M(\tau), q_1(\tau), q_2(\tau))\in\mathbb{H}_\varepsilon\}}\mathrm{d}\tau + \\
&\liminf_{t\to+\infty} \frac{1}{t}\int_0^t \mathbb{E}\left[F_1(P(\tau), M(\tau), q_1(\tau), q_2(\tau))\right] 1_{\{(P(\tau), M(\tau), q_1(\tau), q_2(\tau))\in(\mathbb{R}^2_+\times\mathbb{R}^2\setminus\mathbb{H}_\varepsilon)\}}\mathrm{d}\tau \le \\
&G_1 \liminf_{t\to+\infty} \frac{1}{t}\int_0^t 1_{\{(P(\tau), M(\tau), q_1(\tau), q_2(\tau))\in\mathbb{H}_\varepsilon\}}\mathrm{d}\tau - \liminf_{t\to+\infty} \frac{1}{t}\int_0^t 1_{\{(P(\tau), M(\tau), q_1(\tau), q_2(\tau))\in(\mathbb{R}^2_+\times\mathbb{R}^2\setminus\mathbb{H}_\varepsilon)\}}\mathrm{d}\tau \le \\
&-1 + (G_1 + 1)\liminf_{t\to+\infty} \frac{1}{t}\int_0^t 1_{\{(P(\tau), M(\tau), q_1(\tau), q_2(\tau))\in\mathbb{H}_\varepsilon\}}\mathrm{d}\tau.
\end{aligned} \tag{4.24}$$

From Eqs (4.23) and (4.24), we obtain

$$\liminf_{t\to+\infty} \frac{1}{t}\int_0^t 1_{\{(P(\tau), M(\tau), q_1(\tau), q_2(\tau))\in\mathbb{H}_\varepsilon\}}\mathrm{d}\tau \ge \frac{1}{G_1 + 1} > 0 \text{ a.s.} \tag{4.25}$$

According to the definition of probabilistic events and Fatou's lemma [17], Eq (4.25) is equivalent to

$$\lim_{t\to+\infty}\inf\frac{1}{t}\int_0^t \mathbb{P}(\tau,P(\tau),M(\tau),q_1(\tau),q_2(\tau),\mathbb{H}_\varepsilon)\,d\tau \geq \frac{1}{G_1+1} > 0 \text{ a.s.}, \tag{4.26}$$

where $\mathbb{P}(\tau,P,M,q_1,q_2,\mathbb{H}_\varepsilon)$ is the transition probability of $(P(t),M(t),q_1(t),q_2(t))$ belonging to set $\mathbb{H}_\varepsilon$. In summary, Condition (2) holds. Combined with Lemma 4.1, it follows that Model (2.4) has at least one stationary distribution on ${\mathbb{R}_+}^2\times\mathbb{R}^2$.

Remark 4.1. *Theorem 4.1 reveals the critical conditions under which a population reaches a stationary distribution, offering important ecological insights. Analysis shows that as the patch connectivity parameters D_1 and D_2 increase, $2\sqrt{D_1D_2}-\bar{k}-\bar{d}_*-\sigma_1/\sqrt{\pi\alpha_1}-\sigma_2/\sqrt{\pi\alpha_2}>0$, becomes easier to satisfy; the ecological implications of this result are consistent with the conclusion of Theorem 5.1.*

Remark 4.2. *To further analyze the impact of environmental fluctuations on species survival, the results show that when the intensity of environmental disturbances ($\sigma_i, i=1,2$) decreases or the rate of environmental recovery ($\alpha_i, i=1,2$) increases, condition $2\sqrt{D_1D_2}-\bar{k}-\bar{d}_*-\sigma_1/\sqrt{\pi\alpha_1}-\sigma_2/\sqrt{\pi\alpha_2}>0$, is more easily satisfied, indicating that the population is more likely to converge to a stationary distribution. This quantitative relationship reveals, from the opposite perspective, the adverse effects of environmental fluctuations on species survival: Increase in disturbances weaken a population's ability to cope with environmental pressures, thereby raising the risk of local extinction. Therefore, in conservation practice, in addition to improving habitat quality and connectivity between habitat patches, efforts should also focus on enhancing the system's capacity to buffer against environmental fluctuations—for example, through measures such as maintaining habitat heterogeneity and reducing human disturbance—in order to increase populations' resilience to disturbances and their long-term survival probability.*

5. Extinction

Theorem 5.1. *For any given initial value $(P(0),M(0),q_1(0),q_2(0))^T\in\mathbb{R}_+^2\times\mathbb{R}^2$, if*

$$H=r-\mu+\max\left\{\frac{\sigma_1}{2\sqrt{\pi\alpha_1}},\frac{\sigma_2}{2\sqrt{\pi\alpha_2}}\right\}+\frac{\sigma_1}{\sqrt{2\alpha_1}}+\frac{\sigma_2}{\sqrt{2\alpha_2}}<0 \quad a.s.,$$

then both P and M will become extinct, where $r=\max\{a/A,D_2\}$, $\mu=\min\{\bar{k},\bar{d}_*\}$.

Proof. Define $V_1(P,M,q_1,q_2)=\ln(P+M)+c_1q_1^2/(2\alpha_1)+c_2q_2^2/(2\alpha_2)$. Applying Itô's formula to $V_1(P,M,q_1,q_2)$ yields,

$$\begin{aligned}
\mathrm{d}V_1 &= \Big[\frac{\frac{aP}{A+P}-(\bar{k}+q_1)P-bP^2-D_1P+D_2M-(\bar{d}_*+q_2)M+D_1P-D_2M}{P+M}\Big]\mathrm{d}t\\
&\quad+\frac{c_1\sigma_1^2}{2\alpha_1}\mathrm{d}t+\frac{c_2\sigma_2^2}{2\alpha_2}\mathrm{d}t-c_1q_1^2\mathrm{d}t-c_2q_2^2\mathrm{d}t+\frac{c_1\sigma_1q_1}{\alpha_1}\mathrm{d}B_1(t)+\frac{c_2\sigma_2q_2}{\alpha_2}\mathrm{d}B_2(t)\\
&\leq \Big[\frac{\frac{a}{A}P+D_2M-\bar{k}P-\bar{d}_*M-q_1P-q_2M}{P+M}\Big]\mathrm{d}t+\frac{c_1\sigma_1^2}{2\alpha_1}\mathrm{d}t+\frac{c_2\sigma_2^2}{2\alpha_2}\mathrm{d}t+\frac{c_1\sigma_1q_1}{\alpha_1}\mathrm{d}B_1(t)+\frac{c_2\sigma_2q_2}{\alpha_2}\mathrm{d}B_2(t)\\
&\leq \Big[\frac{r(P+M)-\mu(P+M)+\max\{(-q_1\vee0),(-q_2\vee0)\}(P+M)}{P+M}\Big]dt\\
&\quad+\frac{c_1\sigma_1^2}{2\alpha_1}dt+\frac{c_2\sigma_2^2}{2\alpha_2}dt+\frac{c_1\sigma_1q_1}{\alpha_1}dB_1(t)+\frac{c_2\sigma_2q_2}{\alpha_2}dB_2(t),
\end{aligned}\tag{5.1}$$

where $r = \max\{a/A, D_2\}$, $\mu = \min\{\bar{k}, \bar{d}_*\}$. Next, we review the last two equations of Model (2.4): $\mathrm{d}q_i(t) = -\alpha_i q_i \mathrm{d}t + \sigma_i \mathrm{d}B_i(t)$ $(i = 1, 2)$. As $t \to \infty$, q_i is ergodic [18]. Similar to the proof method in [19], q_i will weakly converge to the invariant density function

$$\omega_i(q) = \frac{\sqrt{\alpha_i}}{\sqrt{\pi}\sigma_i} \mathrm{e}^{-\frac{\alpha_i}{\sigma_i^2} q^2} \ (q \in \mathbb{R}; i = 1, 2).$$

Combining the ergodic theorem [18], we have

$$\int_{-\infty}^{\infty} (-q_i \vee 0)\omega_i(q)\mathrm{d}q = \int_{-\infty}^{0} \frac{(-q)\sqrt{\alpha_i}}{\sqrt{\pi}\sigma_i} \mathrm{e}^{-\frac{\alpha_i q^2}{\sigma_i^2}} \mathrm{d}q = \frac{\sigma_i}{2\sqrt{\pi\alpha_i}} \int_0^{\infty} \mathrm{e}^{-\left(\frac{\sqrt{\alpha_i} q}{\sigma_i}\right)^2} \mathrm{d}\left(\frac{\sqrt{\alpha_i} q}{\sigma_i}\right)^2 = \frac{\sigma_i}{2\sqrt{\pi\alpha_i}}. \tag{5.2}$$

Let $c_1 = \sqrt{2\alpha_1}/\sigma_1$,$c_2 = \sqrt{2\alpha_2}/\sigma_2$. Integrating both sides of Eq (5.1) simultaneously over $[0, t]$ and dividing by t ,we have

$$\begin{aligned} V_1(P(t), M(t), q_1(t), q_2(t))/t \le V_1(P(0), M(0), q_1(0), q_2(0))/t + \frac{\sigma_1}{\sqrt{2\alpha_1}} + \left(\int_0^t \frac{\sqrt{2}q_1}{\sqrt{\alpha_1}} \mathrm{d}B_1(s)\right)/t + \\ r - \mu + \frac{\sigma_2}{\sqrt{2\alpha_2}} + \left(\int_0^t \frac{\sqrt{2}q_2}{\sqrt{\alpha_2}} \mathrm{d}B_2(s)\right)/t + \left(\int_0^t \max\{-q_1(s) \vee 0, -q_2(s) \vee 0\} \mathrm{d}s\right)/t. \end{aligned} \tag{5.3}$$

Combining $\ln(P + M) \le V_1(P, M, q_1, q_2)$ and the strong law of large numbers, we know

$$\lim_{t\to+\infty} \left(\int_0^t \frac{\sqrt{2}q_1}{\sqrt{\alpha_1}} \mathrm{d}B_1(s)\right)/t = 0, \ \lim_{t\to+\infty} \left(\int_0^t \frac{\sqrt{2}q_2}{\sqrt{\alpha_2}} \mathrm{d}B_2(s)\right)/t = 0.$$

As $t \to +\infty$, taking the upper limit on both sides of Eq (5.3) gives

$$\limsup_{t\to+\infty} \frac{\ln(P + M)}{t} \le \limsup_{t\to+\infty} \frac{\ln(P + M) + c_1 q_1^2/2\alpha_1 + c_2 q_2^2/2\alpha_2}{t} \le$$

$$\max\left\{\int_{-\infty}^{\infty} (-q \vee 0)\omega_1(q)\mathrm{d}q, \int_{-\infty}^{\infty} (-q \vee 0)\omega_2(q)\mathrm{d}q\right\} + r - \mu + \frac{\sigma_1}{\sqrt{2\alpha_1}} + \frac{\sigma_2}{\sqrt{2\alpha_2}} =$$

$$r - \mu + \max\left\{\frac{\sigma_1}{2\sqrt{\pi\alpha_1}}, \frac{\sigma_2}{2\sqrt{\pi\alpha_2}}\right\} + \frac{\sigma_1}{\sqrt{2\alpha_1}} + \frac{\sigma_2}{\sqrt{2\alpha_2}} < 0.$$

Thus, $\lim_{t\to+\infty} P(t) = 0$ and $\lim_{t\to+\infty} M(t) = 0$ hold almost everywhere. Consequently, both P and M will become extinct.

Remark 5.1. *Theorem 5.1 reveals the essential conditions for the continued survival of a population and offers important ecological implications. The analysis indicates that an increase in either the intrinsic growth potential (a/A) or the degree of patch connectivity (D_2) reduces the likelihood that condition $H < 0$ will be met, thereby lowering the population's risk of extinction. Therefore, conservation strategies should focus on two primary aspects: First, enhance the population's intrinsic growth capacity by improving habitat quality and increasing resource availability to boost the parameter a/A. Second, enhance connectivity between patches—for example, by establishing ecological corridors—to increase the D_2 parameter, thereby promoting individual migration and gene flow and enhancing population stability.*

□

6. Numerical methods and theoretical justification

As numerical simulation has become a standard method for verifying theoretical results, related advanced algorithms have also developed rapidly [20]. The stochastic differential equation model studied in this paper strictly satisfies the global Lipschitz condition and the linear growth constraint in Lemma 4.1, and meets the corresponding Lyapunov-type stability conditions. This model structure provides a comprehensive theoretical foundation for the standard Euler–Maruyama numerical method. First, the global Lipschitz continuity and linear growth properties of the drift and diffusion terms form the core prerequisites for the strong convergence of the classical Euler–Maruyama method, ensuring that the numerical solution converges strongly to the true solution at a rate of order $1/2$ as the step size approaches zero. Second, Lyapunov-type conditions ensure that the moments of the stochastic process are bounded and that the process is path-stable, effectively avoiding the divergence or blow-up issues that may arise during long-term iterations in numerical simulations [21]. Compared to complex formats such as truncated EM [22], which are designed to address superlinear coefficients, the standard EM method not only offers a more concise and computationally efficient approach in the context of this system, but also benefits from a more mature and comprehensive theory of convergence and stability. Therefore, selecting the standard EM method for numerical simulation—which combines theoretical rigor with computational practicality—is a reasonable and reliable technical approach for verifying the theory derived in this paper.

All numerical simulation results are directly generated using the Euler–Maruyama method. By applying the Euler–Maruyama method , we derive the discretized form of Model (2.4) as follows:

$$\begin{cases} q_1^{j+1} = q_1^j - \alpha_1 q_1^j \Delta t + \sigma_1 \sqrt{\Delta t}\omega_j, \\ q_2^{j+1} = q_2^j - \alpha_2 q_2^j \Delta t + \sigma_2 \sqrt{\Delta t}\xi_j, \\ P^{j+1} = P^j + \left[\frac{aP^j}{A+P^j} - \left(q_1^j + \bar{k}\right) P^j - b(P^j)^2 - D_1 P^j + D_2 M^j\right] \Delta t, \\ M^{j+1} = M^j + \left[-\left(q_2^j + \bar{d}_*\right) M^j + D_1 P^j - D_2 M^j\right] \Delta t, \end{cases} \tag{6.1}$$

Where $\Delta t > 0$ represents the time increment; ω_j, ξ_j are independent stochastic variables following the standard Gaussian distribution $\mathbb{N}(0, 1)$; (q_1^j, q_2^j, P^j, M^j) corresponds to the values obtained at the jth iteration; and the non-negativity constraint is set as $P^{j+1} = \max(P^{j+1}, 0)$, $M^{j+1} = \max(M^{j+1}, 0)$ to ensure biological rationality. We will use different combinations of the biological parameters in Tables 2 and 3 for simulation.

Example 6.1. Set the initial values for Model (2.4) as $P(0) = 1.0$, $M(0) = 0.5$, $q_1(0) = 0$, and $q_2(0) = 0$. Select the combination $(\mathcal{A}_1)$–$(\mathcal{A}_3)$ as the parameter values for Model (2.4), and perform numerical simulations using R to obtain Figure 1. The results of the numerical simulations indicate that the stochastic two-patch system (2.4) has a global solution, thereby verifying Theorem 3.1. The red and blue lines in Figure 1 represent the trends of $P(t)$ and $M(t)$, respectively, whose mortality rates are subject to disturbances from an Ornstein–Uhlenbeck process. These results further confirm the conclusion of Theorem 3.1.

Example 6.2. In Figure 2, the 100 simulation paths are displayed as gray lines, and the green solid line represents their average trajectory. It is observable that varying coefficient combinations result in distinct solutions, and each solution exists uniquely. This confirms the conclusion of Theorem 3.1 .

Example 6.3. Set the initial values for Model (2.4) as $P(0) = 1.0$, $M(0) = 0.5$, $q_1(0) = 0$, and $q_2(0) = 0$. Select combination ($\mathcal{A}_4$) as the parameter values for Model (2.4), and perform a numerical simulation using R to obtain Figure 3. The four figures in Figure 3 show the histograms of the solutions for $P(t)$, $M(t)$, $q_1(t)$, and $q_2(t)$, respectively. Numerical simulation results indicate that when $2\sqrt{D_1D_2} - \bar{k} - \bar{d}_* - \sigma_1/\sqrt{\pi\alpha_1} - \sigma_2/\sqrt{\pi\alpha_2} > 0$, $P(t)$ and $M(t)$ approximately follow a normal distribution, that is, Model (2.4) has a stationary distribution , and Theorem 4.1 holds.

As can be seen in Figure 3, the frequency distributions of the populations $P(t)$ and $M(t)$ exhibit a peak in the middle and tails that taper off at both ends, approximating a normal distribution. Biologically speaking, this indicates the long-term trend in the species dispersal systems of the two patches, suggesting that $P(t)$ and $M(t)$ can persist. In other words, assuming Lemma 4.1 holds and that $2\sqrt{D_1D_2} - \bar{k} - \bar{d}_* - \sigma_1/\sqrt{\pi\alpha_1} - \sigma_2/\sqrt{\pi\alpha_2} > 0$, the two populations will continue to grow and eventually reach a stationary state. This result confirms the conclusion of Theorem 4.1.

Example 6.4. In Figure 4, the 100 simulation paths are displayed as gray lines, and the green solid line represents their average trajectory. This confirms the conclusion of Theorem 4.1 .

Example 6.5. Set the initial values for Model (2.4) to $P(0) = 1.0$, $M(0) = 0.5$, $q_1(0) = 0$, and $q_2(0) = 0$. Select combination ($\mathcal{A}_5$) as the parameter values for Model (2.4), and perform a numerical simulation using R to obtain Figure 5. Upon calculation, $H = r - \mu + \max\left\{\sigma_1/(2\sqrt{\pi\alpha_1}), \sigma_2/(2\sqrt{\pi\alpha_2})\right\} + \sigma_1/\sqrt{2\alpha_1} + \sigma_2/\sqrt{2\alpha_2} = -0.0043 < 0$. According to Theorem 5.1, the populations $P(t)$ and $M(t)$ will tend toward extinction. The first figure in Figure 5 shows that the population $P(t)$ goes extinct at $t = 20$, and the population $M(t)$ goes extinct at $t = 26$; this result confirms the conclusion of Theorem 5.1.

7. Numerical simulations

Table 2. List of biological parameters in the two-patch system.

Parameter	Description
α_1	Reversion speed of $q_1(t)$
α_2	Reversion speed of $q_2(t)$
σ_1	Intensity of volatility of $q_1(t)$
σ_2	Intensity of volatility of $q_2(t)$
a	Birth rate of patch-1
A	Density-dependent coefficient of the nonlinear birth rate of patch-1 population
$\bar{k}$	Average natural mortality rate of patch-1
$\bar{d}_*$	Average natural mortality rate of patch-2
b	Intraspecific competition rate of patch-1
D_1	Dispersal rate from patch-1 to patch-2
D_2	Dispersal rate from patch-2 to patch-1

Table 3. Several combinations of biological parameters of the two-patch system.

Combinations	Value
$(\mathcal{A}_1)$	$\alpha_1 = 1.2,\ \alpha_2 = 2,\ \bar{k} = 0.5,\ \bar{d}_* = 0.6,\ \sigma_1 = 0.05,\ \sigma_2 = 0.05,\ a = 3.0,\ A = 2.0,\ b = 1,\ D_1 = 0.05,\ D_2 = 0.1$
$(\mathcal{A}_2)$	$\alpha_1 = 1.51,\ \alpha_2 = 1.61,\ \bar{k} = 0.46,\ \bar{d}_* = 0.22,\ \sigma_1 = 0.05,\ \sigma_2 = 0.05,\ a = 1.0,\ A = 0.5,\ b = 1,\ D_1 = 0.15,\ D_2 = 0.3$
$(\mathcal{A}_3)$	$\alpha_1 = 2,\ \alpha_2 = 1.2,\ \bar{k} = 0.1,\ \bar{d}_* = 0.3,\ \sigma_1 = 0.1,\ \sigma_2 = 0.1,\ a = 1.0,\ A = 0.5,\ b = 1,\ D_1 = 0.05,\ D_2 = 0.1$
$(\mathcal{A}_4)$	$\alpha_1 = 2.1,\ \alpha_2 = 2.1,\ \bar{k} = 0.3,\ \bar{d}_* = 0.2,\ \sigma_1 = 0.5,\ \sigma_2 = 0.1,\ a = 2.0,\ A = 1.0,\ b = 0.1,\ D_1 = 0.5,\ D_2 = 0.51$
$(\mathcal{A}_5)$	$\alpha_1 = 2.885,\ \alpha_2 = 3.6165,\ \bar{k} = 0.25,\ \bar{d}_* = 0.155,\ \sigma_1 = 0.0025,\ \sigma_2 = 0.268,\ a = 1.0,\ A = 20,\ b = 0.1,\ D_1 = 1.0,\ D_2 = 0.05$

Based on the biological significance of the parameters in Table 2 and the actual ecological data set [23], we select zooplankton as an example. First,we determined the value ranges for each system parameter of (2.4). For example, the values of fluctuation intensity $\sigma_i, (i = 1, 2)$ fall within [0, 5]; the values of the mortality rate fall within [0.1, 0.6]; the values of the birth rate fall within [0.042, 0.76] ; and the dispersal rate values fall within [0.14, 4.80]. All parameter combinations in Table 3 are set within the ecologically viable range defined above and further validated against theoretical thresholds. Specifically, parameter combinations $(\mathcal{A}_4)$ and $(\mathcal{A}_5)$ correspond respectively to the existence condition for a stationary distribution $(2\sqrt{D_1D_2} - \bar{k} - \bar{d}_* - \sigma_1/\sqrt{\pi\alpha_1} - \sigma_2/\sqrt{\pi\alpha_2} > 0,)$ in Theorem 4.1 and the extinction condition $(H < 0\ )$ in Theorem 5.1, aiming to systematically verify the accuracy and validity of the theoretical boundaries.

Remark 7.1. *The parameter ranges cited above are derived from the ecological data set in [23]. Specifically, the fluctuation intensity range is informed by typical values in stochastic ecological models [19], the mortality rate range is based on zooplankton mortality data in Table A458 of [23], the birth rate range is based on zooplankton fecundity data in Table A444 of [23], and the dispersal rate range is based on zooplankton dispersal data in Table A476 of [23]. It should be noted that the mortality rate range [0.1, 0.6] integrates data from Table A458 of [23] with the specific characteristics of our model, ensuring biological realism while maintaining consistency with the model's theoretical framework.*

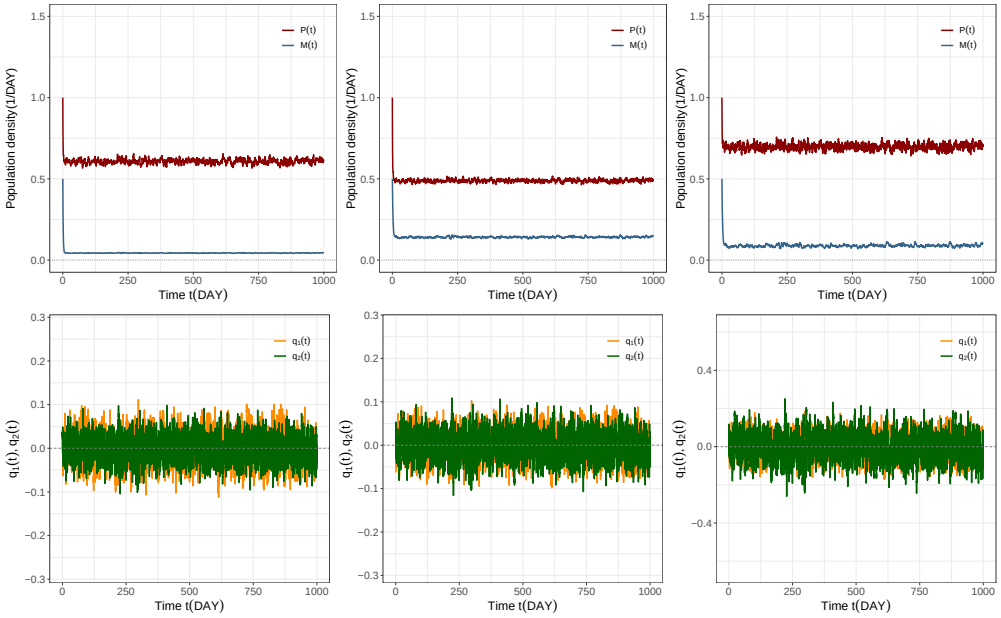

Figure 1. Numerical simulations of the dynamical behavior of patch-1 and patch-2 are performed using parameter combinations ($\mathcal{A}_1$) to ($\mathcal{A}_3$). The simulation results are consistent with Theorem 3.1, confirming the existence and uniqueness of the global solution to the model.

Remark 7.2. *By setting the maximum number of iterations to $T_{max} = 1000$, the results shown in Figure 1 are obtained. The figure shows that the mortality rates of P and M fluctuate around their mean values, reflecting the mean-reverting nature of the Ornstein–Uhlenbeck process. Moreover, different coefficient combinations yield distinct solutions, all of which are existing and unique. These results support the conclusion of Theorem 3.1.*

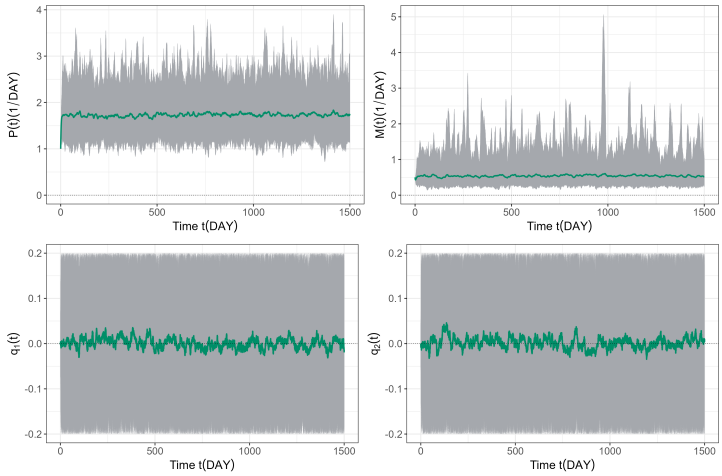

Figure 2. 100-path simulation figures. We perform 100 numerical simulations based on Theorem 3.1. All 100 trajectories are generated with identical initial conditions, parameter settings, and minor random perturbations, where the simulation horizon is set to $T_{\max} = 1500$.

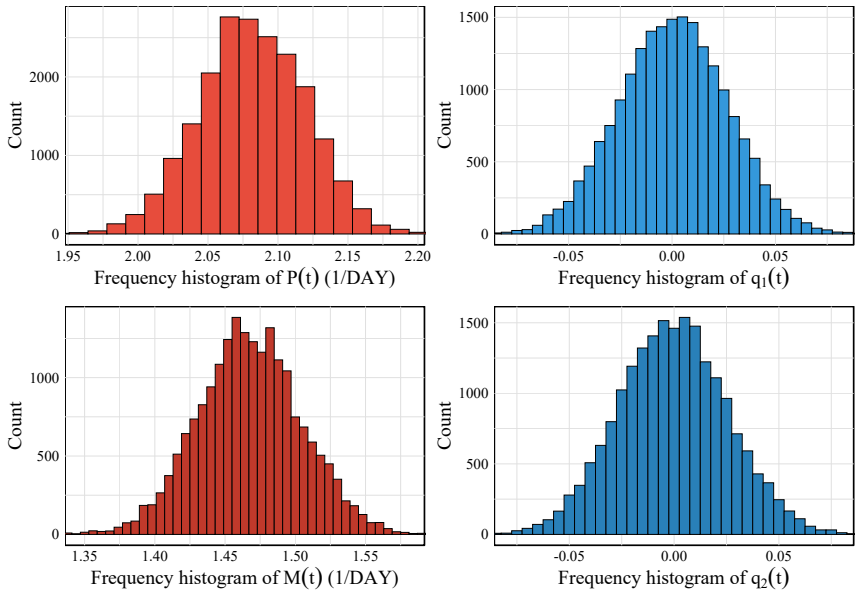

Figure 3. For Model (2.4), parameter combination ($\mathcal{A}_4$) is adopted to define its biological parameters (Table 3), and numerical simulations of its stationary distribution are performed. Theorem 4.1 theoretically ensures the existence of the stationary distribution of the model's solution. Setting the iteration duration to $T = 2000$, the simulation results are presented.

Remark 7.3. *The frequency histograms of $P(t)$, $M(t)$, $q_1(t)$, and $q_2(t)$ exhibit a mode with a high value in the middle and low values at both ends, approximating a normal distribution. Numerical simulations are conducted to study the stationary distribution of Model* (2.4)*, as shown in Figure 3. The total $P(t)$ primarily varies between* 2.03 *and* 2.11*, $q_1(t)$ varies between* -0.03 *and* $+0.03$*, $M(t)$ varies between* 1.43 *and* 1.50*, and $q_2(t)$ varies between* -0.03 *and* $+0.03$*; all variables are concentrated in their respective central ranges. This indicates that, despite random environmental disturbances, the system's dynamics will stabilize.*

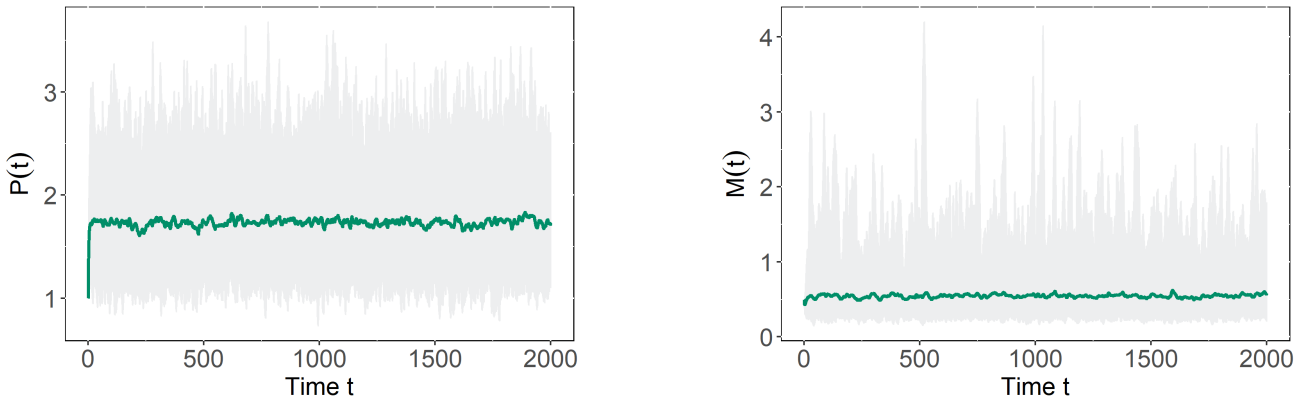

Figure 4. 100-path simulation figures for Theorem 4.1. To further verify Theorem 4.1 , we conduct 100 path simulations using the same methods as in the verification of Theorem 3.1.

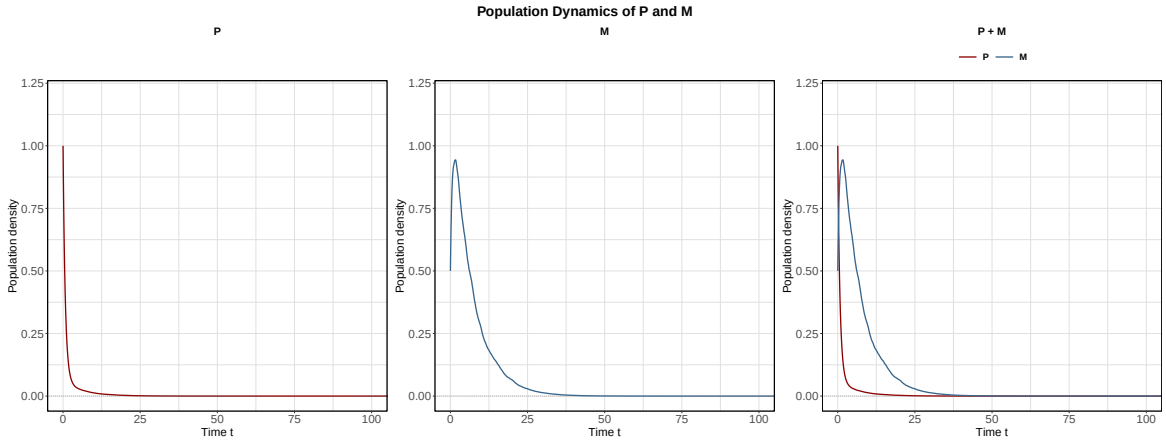

Figure 5. Numerical simulation results indicate that when the condition $H < 0$ is satisfied, the model exhibits extinction behavior: Both the P and M populations tend toward extinction. The parameters adopted in this simulation are determined by combination ($\mathcal{A}_5$) (see Table 3).

8. Conclusions

This paper primarily investigates the mathematical properties of a two-patch model with nonlinear birth rate and dispersal driven by the Ornstein–Uhlenbeck process. First, the existence and uniqueness of the global solution of the model are established. Second, by constructing a Lyapunov function and applying Itô's formula, the existence of the model's stationary distribution is proven.Third, we conclude that the population will go extinct when the condition $H < 0$ is meet where H integrates core parameters, including the patch effective growth rate, dispersal coefficient, intensity of stochastic perturbation, and regulatory parameter of nonlinear birth rate. Finally, numerical simulations are conducted to verify the theoretical results and confirm the validity of the conclusions.

Using zooplankton in aquatic ecosystems as an example, we explain how interpatch diffusion effects, nonlinear birth rates, and Ornstein–Uhlenbeck processes with stochastic mortality fluctuations influence zooplankton survival in real-world ecological settings. From an ecological perspective, selecting zooplankton as a model organism is of great importance. Zooplankton are highly sensitive to environmental changes and can serve as early indicators of ecosystem health. By fitting our stochastic model to the zooplankton data, we have both validated the accuracy of its theoretical predictions and demonstrated its practical applicability.

Finally, this paper explores the ecological implications of these theoretical conditions, offering insights into how habitat fragmentation and environmental noise jointly shape the long-term survival of populations. The model more accurately reflects the random fluctuations and interspecies interactions within ecosystems; the extinction threshold $H < 0$ provides a quantifiable criterion for identifying populations at risk, which can guide early-warning strategies in conservation practice. In summary, this study provides a new theoretical framework for ecological conservation and species management.

Use of AI tools declaration

The authors declare they have not used Artificial Intelligence (AI) tools in the creation of this article.

Acknowledgments

This study was supported by the National Natural Science Foundation of China under Grant (No. 11401085), the Central University Basic Research Grant (2572021DJ04), the Heilongjiang Postdoctoral Grant (LBH-Q21059), the 2023 Year Project on Ideological and Political Education in Graduate Courses of Heilongjiang Province, Northeast Forestry University Educational Teaching Research Project (Graduate Student Special Project, No. DGYYJ2022-22), and the Innovation and Entrepreneurship Training Program for University Students (S202510225029).

Conflict of interest

The authors declare there are no conflicts of interest.

References

1. I. H. Andrén, Effects of habitat fragmentation on birds and mammals in landscapes with different proportions of suitable habitat: A review, *Oikos*, **71** (1994), 355–366. https://doi.org/10.2307/3545823
2. I. Hanski, *Metapopulation Ecology*, Oxford University Press, 1999.
3. C. Grumbach, F. N. Reurik, J. Segura, D. Franco, F. M. Hilker, The effect of dispersal on asymptotic total population size in discrete- and continuous-time two-patch models, *J. Math. Biol.*, **87** (2023), 60. https://doi.org/10.1007/s00285-023-01984-8
4. R. M. May, *Stability and Complexity in Model Ecosystems*, Princeton University Press, Princeton, (2019), 146–157. https://doi.org/10.15789/9780691199121
5. H. L. Wei, W. H. Li, Dynamical behaviors of a Lotka-Volterra competition system with the Ornstein-Uhlenbeck process, *Math. Biosci. Eng.*, **20** (2023), 7882–7904. https://doi.org/10.3934/mbe.2023341
6. X. Liu, H. Cao, L. F. Nie, Insights into infectious diseases with horizontal and environmental transmission: A stochastic model with logarithmic Ornstein-Uhlenbeck process and nonlinear incidence, *Chaos Solitons Fractals*, **191** (2025), 115888. https://doi.org/10.1016/j.chaos.2024.115888
7. H. Wu, Y. S. Wang, Y. F. Li, D. L. DeAngelis, Dispersal asymmetry in a two-patch system with source-sink populations, *Theor. Popul. Biol.*, **131** (2020), 54–65. https://doi.org/10.1016/j.tpb.2019.11.004
8. L. J. Chen, T. T. Liu, F. D. Chen, Stability and bifurcation in a two-patch model with additive Allee effect, *AIMS Math.*, **7** (2022), 536–551. https://doi.org/10.3934/math.2022034
9. S. Tang, L. Chen, Density-dependent birth rate, birth pulses and their population dynamic consequences, *J. Math. Biol.*, **44** (2002), 185–199. https://doi.org/10.1007/s002850100121
10. Q. Yue, Permanence of a delayed biological system with stage structure and density-dependent juvenile birth rate, *Eng. Lett.*, **27** (2019), 1–5.
11. X. Mao, G. Marion, E. Renshaw, Environmental Brownian noise suppresses explosions in population dynamics, *Stochastic Processes Appl.* , **97** (2002), 95–110. https://doi.org/10.1016/S0304-4149(01)00126-0

12. X. Zhang, R. Yuan, A stochastic chemostat model with mean-reverting Ornstein-Uhlenbeck process and Monod-Haldane response function, *Appl. Math. Comput.*, **394** (2021), 125833. https://doi.org/10.1016/j.amc.2020.125833

13. Q. Liu, D. Jiang, Analysis of a stochastic within-host model of dengue infection with immune response and Ornstein-Uhlenbeck process, *J. Nonlinear Sci.*, **34** (2024), 28. https://doi.org/10.1007/s00332-023-10004-4

14. R. Khasminskii, *Stochastic Stability of Differential Equations*, Springer Science & Business Media, Berlin, (2011), 43–58. https://doi.org/10.1007/978-3-642-19947-9

15. R. McVinish, P. K. Pollett, Y. S. Chan, A metapopulation model with Markovian landscape dynamics, *Theor. Popul. Biol.*, **112** (2016), 1–12. https://doi.org/10.1016/j.tpb.2016.08.005

16. D. Y. Xu, Y. M. Huang, Z. G. Yang, Existence theorems for periodic Markov process and stochastic functional differential equations, *Discrete Contin. Dyn. Syst.*, **24** (2009), 1005–1023. https://doi.org/10.3934/dcds.2009.24.1005

17. H. D. Nguyen, H. N. Dang, G. G. Yin, Conditions for permanence and ergodicity of certain stochastic predator-prey models, *J. Appl. Probab.*, **53** (2016), 187–202. https://doi.org/10.1017/jpr.2015.18

18. A. Y. Kutoyants, *Statistical Inference for Ergodic Diffusion Processes*, Springer Science & Business Media, Berlin, (2004), 17–23.

19. Y. Cai, J. Jiao, Z. Gui, Y. Liu, W. Wang, Environmental variability in a stochastic epidemic model, *Appl. Math. Comput.*, **329** (2018), 210–226. https://doi.org/10.1016/j.amc.2018.02.009

20. O. P. Nave, Modification of semi-analytical method applied system of ode, *Mod. Appl. Sci.*, **14** (2020), 75. https://doi.org/10.5539/mas.v14n6p75

21. G. Y. Lv, H. J. Gao, J. L. Wei, J. L. Wu, The effect of noise intensity on parabolic equations, *Discrete Contin. Dyn. Syst. Ser. B*, **24** (2019), 6247–6266. https://doi.org/10.3934/dcdsb.2019248

22. X. R. Mao, The truncated Euler–Maruyama method for stochastic differential equations, *J. Comput. Appl. Math.*, **290** (2015), 370–384. https://doi.org/10.1016/j.cam.2015.06.002

23. S. E. Jørgensen, *Handbook of Environmental Data and Ecological Parameters: Environmental Sciences and Applications*, Pergamon, 1979. https://doi.org/10.1016/C2013-0-05856-2

AIMS Press